

Multiple Stochastic Prompt Tuning for Practical Cross-Domain Few Shot Learning

Debarshi Brahma and Soma Biswas
Indian Institute of Science, Bangalore

Abstract

In this work, we propose a practical cross-domain few-shot learning (pCDFSL) task, where a large-scale pre-trained model like CLIP can be easily deployed on a target dataset. The goal is to simultaneously classify all unseen classes under extreme domain shifts, by utilizing only a few labeled samples per class. The pCDFSL paradigm is source-free and moves beyond artificially created episodic training and testing regimes followed by existing CDFSL frameworks, making it more challenging and relevant to real-world applications. Towards that goal, we propose a novel framework, termed MIST (Multiple Stochastic Prompt tuning), where multiple stochastic prompts are utilized to handle significant domain and semantic shifts. Specifically, multiple prompts are learnt for each class, effectively capturing multiple peaks in the input data. Furthermore, instead of representing the weights of the multiple prompts as point-estimates, we model them as learnable Gaussian distributions with two different strategies, encouraging an efficient exploration of the prompt parameter space, which mitigate overfitting due to the few labeled training samples. Extensive experiments and comparison with the state-of-the-art methods on four CDFSL benchmarks adapted to this setting, show the effectiveness of the proposed framework.

1. Introduction

Cross-domain few-shot learning (CDFSL) aims to adapt a deep learning model to novel classes with only a few labelled examples per class, where the target data has a significant distribution shift from the source data. Existing CDFSL approaches in literature [9, 12, 34] divide the source and target domain datasets into several episodes with fixed number of classes and training examples from each class (commonly known as N-way k-shot setting), to match training and testing conditions. These methods usually involve a resource-intensive meta-training on the source domain episodes followed by finetuning on the target domain episodes. Recent emergence of off-the-shelf large pretrained models like CLIP [24] offers a source-free alternative to replace the complex pretraining stage. Effi-

cient transfer learning (ETL) techniques like prompt tuning [15, 32] have attempted such a setting focusing mainly on datasets with natural images and semantics, overlooking extreme domain shifts or specialized categories. Recently, few works have utilized CLIP for CDFSL [4, 28] for the episodic setup, where the model is fine-tuned on the episodes of the target dataset. However, in real-world, models are usually deployed where all the classes are present together, and rarely on isolated episodes with a few selected classes at a time.

Here, we propose a more realistic setting, practical cross-domain few-shot learning (pCDFSL), inspired by recent work on practical FSL [8], but for the more challenging CDFSL scenario, which unifies the CLIP-based few-shot ETL with the traditional CDFSL paradigms. In pCDFSL, a large-scale pre-trained model after being appropriately tuned using only few labeled samples from all the classes, can directly be deployed to the target dataset with extreme domain shifts. This setting better aligns with real-world deployment needs by enabling simultaneous classification across diverse, unseen classes without the episodic constraints. However, it poses significant challenges, as it involves learning all classes together with few labeled training samples, besides handling complex interactions among classes, leading to harder-to-discriminate class boundaries.

In this work, we propose a novel prompt learning framework for CLIP, termed MIST (Multiple Stochastic Prompt tuning) to address these challenges. Analyzing the existing prompt tuning approaches, we observe that more often than not, unimodal modeling of class-wise data distributions does not hold. In contrast, our multiple prompts are better suited to capture the multimodal class distributions. Moreover, the availability of limited training samples also introduces the risk of overfitting. To this end, unlike standard optimization of prompt weights, here we model the different prompt parameters with different Gaussian distributions represented by learnable mean and variance vectors. This approach facilitates efficient exploration of the prompt parameter space, and prevents overfitting on the few training samples. The key contributions of this work can be summarized as follows:

1. We advocate the practical cross-domain few-shot learn-

ing (pCDFSL) task, which is more realistic and challenging compared to the constrained episodic setting.

2. We extensively evaluate the recent state-of-the-art CLIP-based methods for this task to generate strong baselines.
3. The novel MIST framework introduces multiple prompt vectors to effectively capture the multimodal distributions of the different classes.
4. We propose modeling the weights of the multiple prompts as learnable Gaussian distributions to mitigate overfitting on few samples and improve generalization.
5. Extensive experiments on standard CDFSL benchmarks adapted to this setting, demonstrate the effectiveness of the proposed MIST framework compared to state-of-the-art methods.

2. Related Works

Here, we briefly discuss the related work in literature. **Cross-domain few-shot learning.** The goal of CDFSL is to learn novel categories with a few training examples under large domain shifts. Existing methods in literature can be divided into two categories: meta-learning and transfer learning. Meta-learning approaches [9, 12, 34, 35], typically train a model to learn robust representations over a large number of source domain episodes, and then transfers this model to the target domain episodes. In [12], a simple pipeline with pretrained ViT is introduced, while [9] meta-trains a large-scale pretrained ViT by perturbing the original visual styles. Observing that CLS token of ViTs can absorb domain information, [35] proposes to decouple this information during source-domain training, before adapting on the target domain. [34] implements a new normalization layer to flatten loss landscapes in the representation space. Transfer learning methods [10, 18, 19] propose pre-training the model on source data followed by finetuning it on the target domain episodes. Recently, a few methods [4, 28] have explored adapting vision-language models like CLIP for CDFSL, by direct finetuning on the target episodes. In particular, [28] aims to enhance the robustness of CLIP by mixing domain-invariant text features with image features, while [4] introduces a regularization technique to increase the inter-class margin for enhanced class discrimination. *However, all these approaches rely on the episodic setting, which involves a cumbersome training protocol, making them resource-intensive and impractical for real-world deployment.*

Prompt tuning of VLMs. Recently, vision-language models (VLMs) like CLIP [24] and ALIGN [13], which are pretrained on web-scale data have changed the landscape of computer vision with powerful zero-shot performance. However, adapting such large-scale models to downstream tasks is challenging, due to the risk of overfitting. Efficient transfer learning methods like prompt tuning [15, 16, 32] address this issue by optimizing only a few parameters

added to these models. Specifically, CoOp [32] trains a few prompt vectors appended to the classname text, keeping the CLIP encoders frozen. MaPLe [15] proposes training prompts in both the textual and visual branches to improve multimodal alignment, while PromptSRC [16] further enhances performance by distilling knowledge from the frozen CLIP model. [29] incorporates class description features into the text encoder during prompt tuning to improve discriminability of the classifier. [20] tunes text prompts using a pool of diverse prompts for each class, while [7] adds learnable gaussian noise to each token of the learnable text prompt, to improve generalization. *Our method utilizes a multiple prompt learning framework, whose weights are sampled from different learnable Gaussian distributions to address the pCDFSL task.*

Stochastic neural networks. Standard neural networks train weights deterministically as point-estimates. Contrarily, Bayesian Neural Networks [3, 23] model the weights as probability distributions, making them useful in handling uncertainty in predictions as well as learning robust representations. Stochastic classifiers have been explored in UDA [21], person re-identification [30], incremental learning [14] and DG [33] in prior literature. *To the best of our knowledge, this is the first work which explores stochastic classifiers in the context of CDFSL.*

3. Problem definition and Background

3.1. Practical CDFSL (pCDFSL) paradigm

Traditional CDFSL focuses on classifying novel categories using few samples under distribution shifts in an episodic manner. Let the source and target datasets be denoted as D_{src} and D_{tgt} respectively, which are split into a large number of tasks/ episodes $\mathcal{T} = (\mathcal{S}, \mathcal{Q})$. The support set $\mathcal{S} = \{(X_i, y_i)\}_{i=1}^{N \times k}$ contains k samples from N (typically 5) randomly chosen classes from all the classes in the dataset. The query set $\mathcal{Q} = \{(X_i, y_i)\}_{i=1}^{N \times q}$ contains q samples from the same set of N classes. This setup is commonly termed as the N -way k -shot setting.

In conventional CDFSL, the model is trained on \mathcal{S} followed by evaluation on \mathcal{Q} for each episode of the source dataset D_{src} . The methods are then evaluated based on the average accuracy and the variance over all the episodes of D_{tgt} . Here, we propose a more realistic practical CDFSL (pCDFSL) task, which is characterized as follows:

- 1) **Source-free setup:** A large pre-trained model like CLIP is utilized off-the-shelf, to efficiently leverage the pretrained knowledge base, without any access to source data.
- 2) **Direct deployment:** The model is adapted to the target dataset D_{tgt} using k samples from all the classes simultaneously, instead of only the classes in the current episode. For example, if D_{tgt} consists of C categories, the model is trained on $k \times C$ datapoints.

3) **Realistic evaluation:** The fine-tuned model is tested on the entire test set of D_{tgt} . This is in contrast to the few query samples in each episode (typically 15) in standard CDFSL, which does not reflect the difficulty that may be encountered while deploying models in the wild.

4) **More informative results:** In this setup, the model performance is not dependent on episodic difficulty. In standard CDFSL, some episodes can have less overlap among the class concepts and are easily separable, while others can have semantically similar classes which are difficult to discriminate, often leading to high variance across episodes.

3.2. Preliminaries

Here, we briefly describe the process of classifying images with CLIP and the base network used in this work for completion. Let us denote the CLIP text and image encoders as \mathcal{F}_t and \mathcal{F}_v respectively. The input image $X_v = \mathbb{R}^{C \times H \times W}$ is broken up into patches $\{e_{CLS}, e_1, e_2, \dots, e_M\}$ and fed into the image encoder to extract the image embedding $z_v = \mathcal{F}_v(X_v)$. Similarly, the text input (typically of the form “A photo of a [CLS]”) is tokenized in the form $X_t = \{t_{SOS}, t_1, t_2, \dots, t_{CLS}, t_{EOS}\}$ and fed into the text encoder to get the text embedding $z_t = \mathcal{F}_t(X_t)$. During zero shot classification, the class text embeddings are matched with the image as follows: $\frac{\exp(\langle z_v, z_t \rangle / \tau)}{\sum_{i=1}^C \exp(\langle z_v, z_{t_i} \rangle / \tau)}$,

where C is the number of classes and τ is the temperature constant. The class with highest similarity is the prediction.

Base Network of MIST: In MIST, we employ a multimodal prompt learning strategy, where learnable prompt vectors are appended to the image and textual input branches. Specifically, let the learnable text prompt vectors be denoted as $\theta_t = \{\theta_{t_1}, \theta_{t_2}, \dots, \theta_{t_m}\}$ and the visual prompts as $\theta_v = \{\theta_{v_1}, \theta_{v_2}, \dots, \theta_{v_m}\}$. These are appended to the input text and image patches to form the modified inputs as: $\tilde{X}_t = \{t_{SOS}, \theta_{t_1}, \dots, \theta_{t_m}, t_1, t_2, \dots, t_{CLS}, t_{EOS}\}$ and $\tilde{X}_v = \{e_{CLS}, \theta_{v_1}, \dots, \theta_{v_m}, e_1, e_2, \dots, e_M\}$ respectively. The extracted feature embeddings from the CLIP encoders are now $\tilde{z}_t = \mathcal{F}_t(\tilde{X}_t)$ and $\tilde{z}_v = \mathcal{F}_v(\tilde{X}_v)$. Here, the trainable textual prompts are passed through a learnable projection layer f_ϕ to obtain the visual prompts, i.e., $\theta_v = f_\phi(\theta_t)$. Along with adding prompts to the inputs, we also adopt a deep prompting approach [15, 16], where learnable prompt vectors are attached after every transformer block. When adapting to a downstream task, these multimodal prompts are trained in an end-to-end manner, keeping the CLIP encoders frozen.

4. The Proposed Framework

In pCDFSL, the goal is to efficiently adapt the large-scale pre-trained CLIP using very few samples from all the classes simultaneously, under extreme domain and semantic

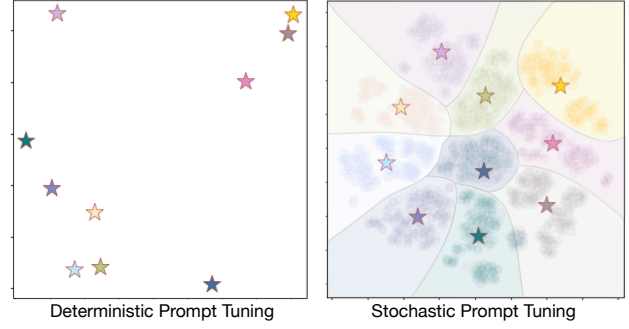


Figure 1. Effect of deterministic vs stochastic prompt learning on the EuroSAT dataset with 1-shot per class. The projected class-specific image features are spread in fixed regions for stochastic learning, implicitly learning well-separated decision boundaries.

Method	EuroSAT	ISIC
1-Shot		
Deterministic Prompt Tuning	73.30	27.50
Stochastic Prompt Tuning (μ, σ^*)	73.43	30.67
Stochastic Prompt Tuning (μ^*, σ^*)	67.40	22.67
8-Shots		
Deterministic Prompt Tuning	86.80	46.53
Stochastic Prompt Tuning (μ, σ^*)	86.73	50.80
Stochastic Prompt Tuning (μ^*, σ^*)	88.03	50.93

Table 1. Stochastic prompt learning with two different sampling techniques on EuroSAT and ISIC. The fixed mean approach (μ, σ^*) performs better in low shots, while sampling from a fully learnable distribution (μ^*, σ^*) performs better in higher shots.

shifts. Towards this goal, we propose two novel additions to the base network to handle different aspects of this setting: (i) Stochastic prompt learning to mitigate the risk of overfitting due to very few training examples and (ii) Multiple prompts to address the implicit unimodal assumption regarding the class data distributions. Together they constitute our final proposed framework, which is illustrated in Figure 3. We describe the motivation and details of the proposed additions next.

4.1. Stochastic Prompt Learning

Although existing prompt tuning methods optimize a few learnable parameters appended to the inputs, the limited availability of training samples makes large-scale models like CLIP prone to overfitting as observed by [16]. While prior methods have addressed this using regularization modules [16] or architectural modifications [15], here we explore a different strategy using stochastic prompt learning to address the overfitting issue.

The main idea is to learn a distribution over the prompt

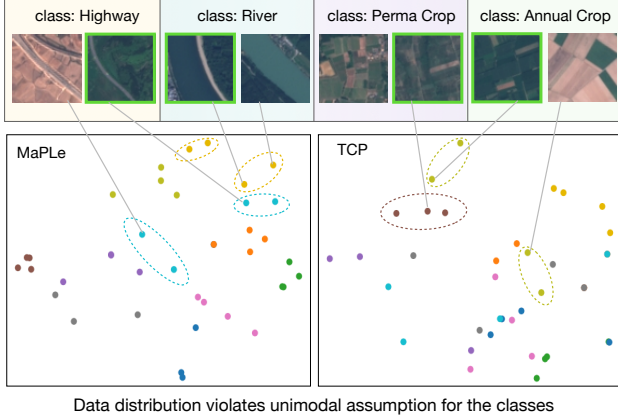


Figure 2. t-SNE visualization of image embeddings from MaPLE [15] (left) and TCP [29] (right) for the EuroSAT dataset. The classwise data distribution violates the unimodal assumption, due to high interclass similarity and intraclass variations.

parameters instead of optimizing them as point-estimates as is the standard practice. This helps to mitigate the uncertainty arising from scarce data, since each distinct sampled weight from this learnable distribution forms diverse decision boundaries for the few shot data, by allowing a richer exploration of the prompt parameter space. This provides an implicit regularization to the model without additional loss functions leading to more robust decision boundaries for the few-shot training samples. Specifically, we sample the text prompt weights from a Gaussian distribution $\mathcal{N}(\mu, \sigma)$, parameterized by mean μ and variance σ as follows: $\theta_t \sim \mathcal{N}(\mu, \sigma)$. After every iteration, we backpropagate the loss to the learnable μ and σ parameters. For end-to-end training, we use the Gaussian reparameterization trick [17] as follows:

$$\theta_t = \mu + \mathcal{N}(0, I) \odot \sigma \quad (1)$$

We illustrate the effect of stochastic prompt learning in Figure 1. In the deterministic case, passing the same examples through the trained model always projects them to the same points in the feature space. In contrast, the projections in the stochastic scenario spreads over a broader region, due to sampling of weights from the learned distribution. This variability implicitly encourages a margin between the class-specific features, resulting in more discriminative decision boundaries.

To verify this phenomenon quantitatively, we consider two distinct strategies for sampling the text prompt parameters. In the first case, we fix the mean of the Gaussian to the standard prompt “A photo”, keeping the variance learnable. In the second case, both the mean and variance are learnable. The results on two representative datasets from the BSCDFSL [10] benchmark are shown in Table 1. We

observe that in the low-shot setting, the first approach outperforms the second, while an opposite trend is seen in the higher-shot setting. This suggests that with very few training data (1-shot), directly optimizing the parameters of a distribution is challenging, but exploring variations around a standard prompt improves performance. On the contrary, learning the full distribution with more data outperforms the fixed mean approach. Hence, the two strategies complement each other in facilitating an efficient coverage of the prompt parameter space.

4.2. MIST: Multiple Stochastic Prompt Tuning

Since CLIP is pretrained on web-scale data encompassing mainly natural images [24], the image encoder struggles to learn robust classwise features when faced with extreme domain and semantic shifts in the target dataset. In addition, intraclass diversity and interclass similarity in the images due to presence of all classes together, results in disjoint clusters in visual features from the same class. Consider an illustrative example of the EuroSAT dataset containing satellite images of various terrains. Here, distinct classes like “Highway” and “River” can have similar visual representatives in the few-shot training data, at the same time featuring diverse visuals from the same classes as shown in Figure 2. Existing prompt tuning approaches represent each class with single learnable prompts, implicitly assuming that classwise visual features form single clusters. However, such a strategy is insufficient to represent the disjoint visual clusters, which may result from such challenging settings. To illustrate this, we consider two representative prompt-tuning methods, MaPLE [15] and TCP [29] and show their t-SNE visualizations in Figure 2. We observe that the unimodal assumption is violated and the image embeddings of each class form multiple modes in the representation space.

To address this, inspired from [1, 2], we introduce a multiple prompt learning approach, where we represent each class with multiple prompt vectors. However, incorporating too many learnable prompts for each class is not desirable since: (i) Each class contains few training samples, and many text embeddings per class could lead to overfitting on individual datapoints, resulting in loss of class level representations, and (ii) it introduces additional learnable parameters and thus more computational overhead. As a balanced approach, we represent each class with two prompt vectors.

Formally, let the embeddings corresponding to the two prompts for a particular class CLS_k be denoted as \tilde{z}_t^i , where, $i = 1, 2$. Here, $\tilde{z}_t^i = \mathcal{F}_t(\tilde{X}_t^i)$, where, $\tilde{X}_t^i = \{t_{SOS}, \theta_t^i, t_1, \dots, t_{CLS_k}, t_{EOS}\}$ is the i^{th} text prompt for the class CLS_k . $\theta_t^i = \{\theta_{t1}^i, \theta_{t2}^i, \dots, \theta_{tm}^i\}$ denotes the i^{th} set of learnable prompt vectors for that particular class.

To simultaneously represent the underlying multimodal class distribution and mitigate overfitting, we stochastically model the parameters of the two prompts for each class as

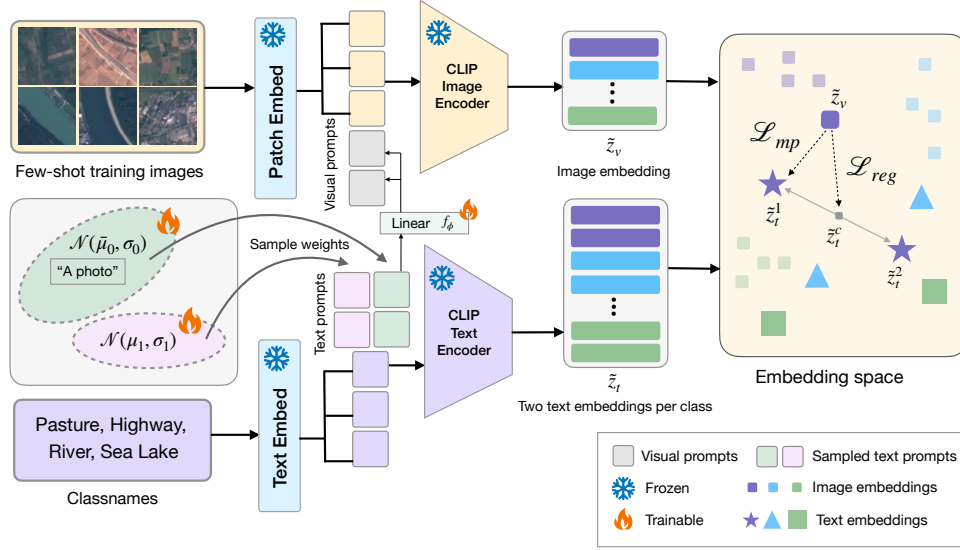


Figure 3. **Our proposed MIST framework.** We append two sets of prompts to the classnames, one sampled from a fixed mean ($\bar{\mu}_0, \sigma_0$) and the other from a fully learnable Gaussian distribution (μ_1, σ_1). f_ϕ projects the text prompts to visual prompts. The loss term \mathcal{L}_{mp} trains the distribution parameters ($\mu_1, \sigma_0, \sigma_1$) and f_ϕ such that the image embedding is assigned to the closest text prototype of its respective class. The \mathcal{L}_{reg} term prevents the two prompts from collapsing by enforcing diversity in the class-wise prompt training.

described in Sec 4.1. Specifically, we incorporate the fixed mean, learnable variance approach on the parameters of the first prompt, simultaneously learning a full Gaussian distribution over the parameters of the second prompt:

$$\begin{aligned} \theta_t^1 &\sim \mathcal{N}(\bar{\mu}_0, \sigma_0) \\ \theta_t^2 &\sim \mathcal{N}(\mu_1, \sigma_1) \end{aligned} \quad (2)$$

Here, $\bar{\mu}_0$ is a fixed vector corresponding to the text embedding of “A photo”, and $\mu_1, \sigma_0, \sigma_1$ are learnable parameters. Now, we describe the training process of MIST.

MIST Training: For a particular image embedding \tilde{z}_v , we first find the closest text embedding of its respective class after every iteration, based on cosine similarity as follows:

$$i^* = \underset{i \in \{1,2\}}{\operatorname{argmax}} \quad \operatorname{sim}(\tilde{z}_t^i, \tilde{z}_v) \quad (3)$$

where, $\operatorname{sim}(a, b) = \frac{a \cdot b}{\|a\| \|b\|}$ denotes the cosine similarity. During training, the image embedding is assigned to its closest prompt embedding by minimizing the following loss function:

$$\mathcal{L}_{mp} = -\log \left(\frac{\exp(\operatorname{sim}(\tilde{z}_t^{i^*}, \tilde{z}_v))}{\sum_{j=1}^{2C} \exp(\operatorname{sim}(\tilde{z}_t^j, \tilde{z}_v))} \right) \quad (4)$$

where, C is the number of classes, and $\operatorname{sim}(\cdot)$ denotes the cosine similarity. To prevent the image embedding \tilde{z}_v from being always assigned to a single text prompt, and encourage diversity when training the two prompts within the same

class, we minimize an additional regularization term to increase the cosine similarity of the image embedding to the centroid of the two text embeddings of its corresponding class:

$$\mathcal{L}_{reg} = -\operatorname{sim}(\tilde{z}_v, \tilde{z}_t^c) \quad (5)$$

where, $\tilde{z}_t^c = \frac{1}{2}(\tilde{z}_t^1 + \tilde{z}_t^2)$ is the centroid of the prompt embeddings for the corresponding class and $\operatorname{sim}(\cdot)$ represents the cosine similarity. Thus, the final objective function is:

$$\mathcal{L}_{total} = \mathcal{L}_{mp} + \mathcal{L}_{reg} \quad (6)$$

This loss function is used to optimize the Gaussian parameters μ_1, σ_0 and σ_1 , as well as the projection layers as:

$$\mu_1^*, \sigma_0^*, \sigma_1^*, \phi^* = \underset{\mu_1, \sigma_0, \sigma_1, \phi}{\operatorname{argmin}} \quad \mathbb{E}_{(X,y) \sim D_{tgt}} \mathcal{L}_{total}(X, y) \quad (7)$$

Inference: Once we learn the parameters of the distribution, during inference, we can now sample weights for the two text prompts as follows: $\theta_t^1 \sim \mathcal{N}(\bar{\mu}_0, \sigma_0^*)$ and $\theta_t^2 \sim \mathcal{N}(\mu_1^*, \sigma_1^*)$. For each class, we take the maximum logit among the two text prompts as the output prediction for that class.

5. Experimental Results

Here, we extensively evaluate the proposed framework and compare it with the state-of-the-art approaches.

Datasets used: The proposed pCDFSL setting is source-free. For the target datasets, we consider the BSCDFSL [10]

Method	EuroSAT	ISIC	PDisease	ChestX	Average
1-shot					
CoOp (IJCV'22) [32]	51.87	22.77	24.73	22.83	30.55
TaskRes (CVPR'23) [31]	64.67	19.70	36.57	10.97	32.98
MaPLe (CVPR'23) [15]	73.30	27.50	51.53	14.60	41.73
PromptSRC (ICCV'23) [16]	73.23	21.97	55.03	14.37	41.15
CLAP (CVPR'24) [25]	61.46	26.61	47.22	15.94	37.81
TCP (CVPR'24) [29]	64.30	27.80	49.37	14.93	39.10
MIST (Ours)	77.90	34.40	50.27	17.10	44.92
2-shots					
CoOp (IJCV'22) [32]	66.00	21.87	37.97	14.43	35.07
TaskRes (CVPR'23) [31]	68.83	23.13	39.27	10.83	35.52
MaPLe (CVPR'23) [15]	78.07	31.90	67.17	16.27	48.35
PromptSRC (ICCV'23) [16]	79.53	29.47	68.07	12.70	47.44
CLAP (CVPR'24) [25]	70.63	34.79	60.13	16.43	45.50
TCP (CVPR'24) [29]	70.37	36.87	62.63	15.63	46.38
MIST (Ours)	81.57	36.37	69.60	13.90	50.36
4-shots					
CoOp (IJCV'22) [32]	66.53	25.00	42.67	17.93	38.03
TaskRes (CVPR'23) [31]	72.40	21.40	39.35	10.27	35.86
MaPLe (CVPR'23) [15]	84.03	37.17	77.07	19.73	54.50
PromptSRC (ICCV'23) [16]	85.23	37.63	78.70	15.17	54.18
CLAP (CVPR'24) [25]	76.43	34.37	65.11	18.98	48.72
TCP (CVPR'24) [29]	76.77	37.37	67.97	17.07	49.80
MIST (Ours)	85.93	40.90	79.67	18.67	56.29
8-shots					
CoOp (IJCV'22) [32]	76.53	38.27	60.50	14.60	47.48
TaskRes (CVPR'23) [31]	74.63	34.30	57.77	12.57	44.82
MaPLe (CVPR'23) [15]	86.80	46.53	84.47	14.17	57.99
PromptSRC (ICCV'23) [16]	88.37	42.47	86.80	14.93	58.14
CLAP (CVPR'24) [25]	76.85	42.81	74.62	14.97	52.31
TCP (CVPR'24) [29]	79.03	46.57	76.33	14.97	54.23
MIST (Ours)	88.63	52.70	87.47	16.50	61.33
16-shots					
CoOp (IJCV'22) [32]	82.83	43.40	69.90	18.80	53.73
TaskRes (CVPR'23) [31]	79.90	38.10	69.40	12.87	50.07
MaPLe (CVPR'23) [15]	92.80	55.53	89.93	13.90	63.04
PromptSRC (ICCV'23) [16]	92.55	55.17	91.40	14.83	63.49
CLAP (CVPR'24) [25]	82.96	49.43	78.27	17.47	57.03
TCP (CVPR'24) [29]	84.93	52.83	80.63	16.53	58.73
MIST (Ours)	93.57	60.30	91.73	14.77	65.09

Table 2. Performance comparison (average accuracy (%) over 3 seeds) of the proposed MIST with the state-of-the-art approaches in the pCDFSL setting for $k = 1, 2, 4, 8, 16$ shots from each class.

benchmark, consisting of four datasets, namely EuroSAT [11], ISIC [5], Plant Disease [22] and ChestX [27]. These datasets cover a varying spectrum of domain shifts, along with specialized classnames, encompassing satellite, agricultural and medical images. For training, we consider few samples ($k = 1, 2, 4, 8, 16$) randomly selected from all the classes together and then evaluate the trained model on the full test set of all the datasets. The final accuracy is taken as the average over 3 different seeds.

Implementation details: We employ CLIP ViT-B/16 as the backbone for our method similar to MaPLe [15]. The learnable context length of the text and vision inputs are set as 2, and deep prompts are incorporated upto a depth of 9. The

model is trained using SGD optimizer for 150 epochs with a learning rate of 0.0035 and a batch size of 4. All experiments are conducted on a NVIDIA RTX A5000 GPU.

5.1. Experiments in the proposed pCDFSL setting

To validate the effectiveness of our approach, we compare our proposed MIST with several recent CLIP-based efficient transfer learning methods for varying number of shots. Specifically, we compare with 1) **CoOp** [32] and **TCP** [29] which employ prompt tuning on the text branch; 2) **MaPLe** [15] and **PromptSRC** [16] which utilizes a multimodal prompt tuning approach; 3) **TaskRes** [31] where task-specific adapters are tuned keeping the base text classifier fixed; 4) **CLAP** [25] uses a linear-probing approach and mainly addresses the absence of validation sets in FSL.

For fair comparison, we run all the methods (using the official, publicly available codes) on the ViT-B/16 backbone and report the results in Table 2. We list some observations here: (i) Among the competing methods, MaPLe and PromptSRC achieves the highest performance on average, closely followed by TCP. Their improved performance suggests the effectiveness of multimodal prompt tuning in handling distribution shifts over text prompt tuning, which was also observed in [15]. This observation is further supported by our results; (ii) Although, CLAP is a recent approach, it mainly focuses on the validation problem of FSL. The reduced performance of CLAP highlights the limitations of linear probing, which does not utilize the text information for handling significant semantic and domain shifts; (iii) As the number of shots increases, the multimodal prompt tuning approaches like MaPLe, PromptSRC and MIST outperforms other methods by larger margins, suggesting that training more parameters is more effective for higher shots. (iv) Although all the methods show similar performance on the ChestX dataset, their overall accuracies are extremely low due to the large domain shift. However, text prompt tuning methods perform slightly better than the multimodal counterparts. This maybe because ChestX contains greyscale images, where additional prompt tuning in the vision branch degrades the performance. Overall, our proposed MIST framework outperforms the other methods significantly, giving consistent average gains of 3.19%, 2.01%, 1.79%, 3.19%, 1.60% on $k = 1, 2, 4, 8, 16$ shots respectively, over the best performing methods. The significant improvement for the 1-shot case highlights the effectiveness of our approach in mitigating overfitting in extremely low data scenarios.

5.2. Additional Analysis

Here we perform additional analysis and ablation studies to further validate our proposed framework. For the analysis, we compare with MaPLe, PromptSRC since they use multimodal prompts and are better suited for the pCDFSL

Dataset	MaPLE	PromptSRC	TCP	MIST (Ours)
EuroSAT	72.90	74.10	57.80	76.90
ISIC	14.80	16.10	13.13	16.73

Table 3. Performance comparison (%) of MIST with state-of-the-art methods on the class-imbalanced setting, with varying data samples from each class.

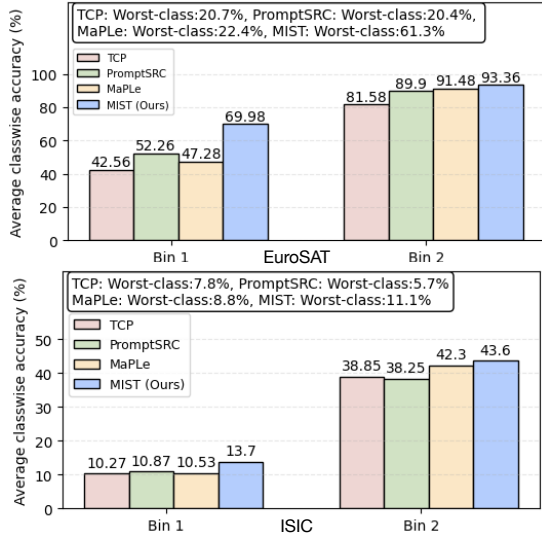


Figure 4. Generalization to classes: The class-wise accuracies are sorted and divided into 2 bins. Our proposed MIST outperforms the other methods in both the bins and also increases the worst-class accuracy for the same seed in the challenging 1-shot setting.

task and TCP, since it is the state-of-the-art prompt tuning approach on CLIP.

1) Class-imbalanced learning: Here, we explore an even more challenging and realistic scenario, where the proposed pCDFSL setting may have varying training data from individual classes. The standard few-shot settings in literature assume an idealistic scenario where each class has exactly k training samples, overlooking the effect of class imbalance. To create such a setting, we perform data sampling in a cyclic manner, e.g., we take $\{1, 2, 4, 8, 1, 2, \dots\}$ from each class of the target dataset for training. The model is then evaluated on the entire test set. The results on two representative datasets, EuroSAT and ISIC in Table 3 shows that the proposed MIST outperforms the other methods even under class-imbalanced conditions, highlighting its effectiveness.

2) Sensitivity to training samples: The representation learning capability of a model is largely influenced by the *few* sampled training examples across classes. However, a robust model should ideally achieve a lower variance

		EuroSAT	ISIC
1-shot	MaPLE	73.30 \pm 3.84	27.50 \pm 10.19
	PromptSRC	73.23 \pm 3.75	21.97 \pm 6.09
	TCP	64.30 \pm 3.24	27.80 \pm 6.55
	MIST (Ours)	77.90 \pm 2.63	34.40 \pm 3.56
2-shots	MaPLE	78.07 \pm 5.87	31.90 \pm 6.08
	PromptSRC	79.53 \pm 2.76	29.47 \pm 6.50
	TCP	70.37 \pm 2.31	36.87 \pm 8.29
	MIST (Ours)	81.57 \pm 1.84	36.37 \pm 3.96

Table 4. The proposed MIST has much lower variance across three different random seeds compared to the other approaches.

across different sampling strategies. To account for this, all the reported results are accuracies averaged over 3 different random seeds. Here, we further report the variance across the 3 seeds for the EuroSAT and ISIC datasets in Table 4. We observe that the proposed MIST not only achieves a higher accuracy, but also shows a much lower variance, highlighting its robustness to different sampling techniques.

3) Generalization to all classes: In practical scenarios, the overall accuracy is often not a reliable metric to understand the model’s ability to represent difficult classes. Here, we study the effectiveness of our multiple stochastic prompt-tuning approach in learning generalized class boundaries and modeling all the complex class distributions. Specifically, we first sort the class-wise accuracies in ascending order. The classes are then divided into two bins in this order to highlight the gain in accuracy in both the lower as well as the higher bin. The comparison with the other methods are shown in Figure 4 for one random seed (same for all methods). We observe that the proposed MIST improves the accuracies in both the bins, while also increasing the worst-class accuracy, which indicates that MIST learns more generalized class representations.

4) Ablation Study: Our proposed MIST framework models the two text classifiers using two distinct Gaussian sampling techniques as described earlier. Here we analyze the effectiveness of each of the proposed components in Table 5. Our base method is the existing multimodal prompt tuning framework, i.e., MaPLE. Introducing stochasticity to this single prompt (fixed mean) tuning approach by sampling from a learnable Gaussian distribution mitigates overfitting as described earlier, and improves the performance. Introducing the second learnable text prompt sampled from a fully learnable distribution without the \mathcal{L}_{reg} term increases performance in EuroSAT, but reduces for ISIC. This can happen due to collapse of the two classifiers without the regularization term [1, 26]. Finally, adding the regularization term \mathcal{L}_{reg} outperforms the baseline significantly for both the datasets.

Method	EuroSAT	ISIC
Base Network	73.30	27.50
+ Stochastic Prompt Learning (μ, σ^*)	73.43	30.67
+ Multiple Stochastic Prompting	74.27	27.00
+ Multiple Stochastic Prompting + \mathcal{L}_{reg} (MIST)	77.90	34.40

Table 5. Ablation study (1-shot): Each proposed component contributes to the impressive performance of the proposed framework.

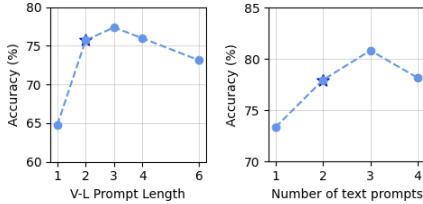


Figure 5. Effect of prompt length (left) and number of text prompts per class (right). We report results for the EuroSAT (1-shot) case.

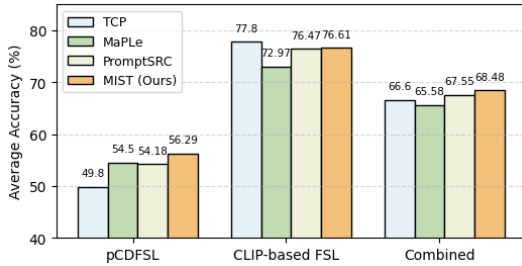


Figure 6. Average accuracies for the pCDFSL and CLIP-based FSL benchmark datasets for the 4-shot setting. MIST outperforms other methods in the pCDFSL setting, and is second to TCP in FSL. Overall, MIST performs better on all the datasets combined.

Number of text prompts & Prompt Length: MIST utilizes two prompts per class sampled from learnable Gaussian distributions. Here we study the effect of adding more text prompts to our approach. For this, we keep one prompt with a fixed mean, and all the others sampled from fully learnable distributions.

From Figure 5 (right), we observe that the performance starts decreasing after three prompts, suggesting overfitting from the increasing number of learnable parameters. Further, addition of more classifiers introduces increased computational overhead and longer training time. The effect of increasing the number of learnable prompt vectors is illustrated in Figure 5 (left). Here also, the accuracy decreases after a point, indicating overfitting in the few-shot setting. We have used 2 learnable prompts for all the experiments.

Qualitative Results: We illustrate the inherent challenges of these datasets in Figure 7, along with some of the predictions from the proposed MIST framework.

5) Future Directions: Existing CDFSL methods in liter-

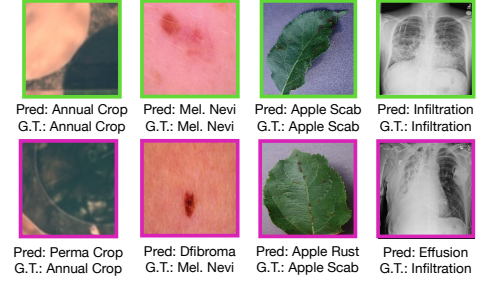


Figure 7. Qualitative results: From left to right, shows predictions on EuroSAT, ISIC, Plant Disease and ChestX respectively. Green denotes correct while red denotes incorrect predictions.

ature typically do not evaluate on natural image datasets and FSL methods do not test on significant domain shifts. However, it is important for the research community to develop more generalized frameworks which work across diverse semantics and distribution shifts seamlessly. Although MIST is designed to address the pCDFSL task, we study its effect on natural image datasets with simpler domain or semantic shifts. For this, we consider the CLIP-based FSL datasets like DTD, Caltech101, Oxford Pets, Flowers, Aircraft, Food101. From Figure 6, we observe that the proposed MIST is only second to the state-of-the-art TCP [29] on average for these datasets and outperforms all the other approaches. It is worth mentioning that unlike MIST, 1) TCP and PromptSRC utilizes detailed class descriptions to incorporate prior knowledge, which requires handcrafting well-designed prompts; 2) they also require the zero-shot CLIP model, resulting in increased memory consumption. Overall, the proposed MIST outperforms all the other methods on average when considered across all datasets encompassing both natural and domain-shifted images and classnames, as observed in Figure 6.

6. Conclusion

In this work, we advocate a more realistic and challenging setting termed as the practical CDFSL (pCDFSL) setting, where a large-scale model like CLIP is adapted to a few-shot downstream dataset without the episodic constraints. We further propose a novel prompt tuning approach, MIST to address the various challenges of this setting. Different from existing prompt tuning approaches, our proposed MIST learns multiple text prompts per class, modeled by distinct learnable Gaussian distributions to represent the inherent multimodal class distributions as well as mitigate overfitting. Extensive experiments on the proposed pCDFSL setting as well as additional analysis show the effectiveness of our proposed approach compared to state-of-the-art methods.

References

- [1] Arman Afrasiyabi, Jean-François Lalonde, and Christian Gagné. Mixture-based feature space learning for few-shot image classification. In *Proceedings of the IEEE/CVF international conference on computer vision*, pages 9041–9051, 2021. 4, 7
- [2] Kelsey Allen, Evan Shelhamer, Hanul Shin, and Joshua Tenenbaum. Infinite mixture prototypes for few-shot learning. In *International conference on machine learning*, pages 232–241. PMLR, 2019. 4
- [3] Charles Blundell, Julien Cornebise, Koray Kavukcuoglu, and Daan Wierstra. Weight uncertainty in neural network. In *International conference on machine learning*, pages 1613–1622. PMLR, 2015. 2
- [4] Debarshi Brahma, Anuska Roy, and Soma Biswas. Prompt tuning vision language models with margin regularizer for few-shot learning under distribution shifts. *Transactions on Machine Learning Research*. 1, 2
- [5] Noel Codella, Veronica Rotemberg, Philipp Tschandl, M Emre Celebi, Stephen Dusza, David Gutman, Brian Helba, Aadi Kalloo, Konstantinos Liopyris, Michael Marchetti, et al. Skin lesion analysis toward melanoma detection 2018: A challenge hosted by the international skin imaging collaboration (isic). *arXiv preprint arXiv:1902.03368*, 2019. 6, 11
- [6] Jia Deng, Wei Dong, Richard Socher, Li-Jia Li, Kai Li, and Li Fei-Fei. Imagenet: A large-scale hierarchical image database. In *2009 IEEE conference on computer vision and pattern recognition*, pages 248–255. Ieee, 2009. 11
- [7] Mohammad Mahdi Derakhshani, Enrique Sanchez, Adrian Bulat, Victor G Turrissi da Costa, Cees GM Snoek, Georgios Tzimiropoulos, and Brais Martinez. Bayesian prompt learning for image-language model generalization. In *Proceedings of the IEEE/CVF International Conference on Computer Vision*, pages 15237–15246, 2023. 2
- [8] Minghao Fu and Ke Zhu. Instance-based max-margin for practical few-shot recognition. In *Proceedings of the IEEE/CVF Conference on Computer Vision and Pattern Recognition*, pages 28674–28683, 2024. 1
- [9] Yuqian Fu, Yu Xie, Yanwei Fu, and Yu-Gang Jiang. Styleadv: Meta style adversarial training for cross-domain few-shot learning. In *Proceedings of the IEEE/CVF Conference on Computer Vision and Pattern Recognition*, pages 24575–24584, 2023. 1, 2
- [10] Yunhui Guo, Noel C Codella, Leonid Karlinsky, James V Codella, John R Smith, Kate Saenko, Tajana Rosing, and Rogerio Feris. A broader study of cross-domain few-shot learning. In *Computer Vision—ECCV 2020: 16th European Conference, Glasgow, UK, August 23–28, 2020, Proceedings, Part XXVII 16*, pages 124–141. Springer, 2020. 2, 4, 5, 11
- [11] Patrick Helber, Benjamin Bischke, Andreas Dengel, and Damian Borth. Eurosat: A novel dataset and deep learning benchmark for land use and land cover classification. *IEEE Journal of Selected Topics in Applied Earth Observations and Remote Sensing*, 12(7):2217–2226, 2019. 6, 11
- [12] Shell Xu Hu, Da Li, Jan Stühmer, Minyoung Kim, and Timothy M Hospedales. Pushing the limits of simple pipelines for few-shot learning: External data and fine-tuning make a difference. In *Proceedings of the IEEE/CVF Conference on Computer Vision and Pattern Recognition*, pages 9068–9077, 2022. 1, 2
- [13] Chao Jia, Yinfei Yang, Ye Xia, Yi-Ting Chen, Zarana Parekh, Hieu Pham, Quoc Le, Yun-Hsuan Sung, Zhen Li, and Tom Duerig. Scaling up visual and vision-language representation learning with noisy text supervision. In *International conference on machine learning*, pages 4904–4916. PMLR, 2021. 2
- [14] Jayateja Kalla and Soma Biswas. S3c: Self-supervised stochastic classifiers for few-shot class-incremental learning. In *European Conference on Computer Vision*, pages 432–448. Springer, 2022. 2
- [15] Muhammad Uzair Khattak, Hanoona Rasheed, Muhammad Maaz, Salman Khan, and Fahad Shahbaz Khan. Maple: Multi-modal prompt learning. In *Proceedings of the IEEE/CVF Conference on Computer Vision and Pattern Recognition*, pages 19113–19122, 2023. 1, 2, 3, 4, 6, 11
- [16] Muhammad Uzair Khattak, Syed Talal Wasim, Muzammal Naseer, Salman Khan, Ming-Hsuan Yang, and Fahad Shahbaz Khan. Self-regulating prompts: Foundational model adaptation without forgetting. In *Proceedings of the IEEE/CVF International Conference on Computer Vision*, pages 15190–15200, 2023. 2, 3, 6, 11
- [17] Diederik P Kingma, Max Welling, et al. Auto-encoding variational bayes, 2013. 4
- [18] Hanwen Liang, Qiong Zhang, Peng Dai, and Juwei Lu. Boosting the generalization capability in cross-domain few-shot learning via noise-enhanced supervised autoencoder. In *Proceedings of the IEEE/CVF international conference on computer vision*, pages 9424–9434, 2021. 2
- [19] Bingyu Liu, Zhen Zhao, Zhenpeng Li, Jianan Jiang, Yuhong Guo, and Jieping Ye. Feature transformation ensemble model with batch spectral regularization for cross-domain few-shot classification. *arXiv preprint arXiv:2005.08463*, 2020. 2
- [20] Yuning Lu, Jianzhuang Liu, Yonggang Zhang, Yajing Liu, and Xinmei Tian. Prompt distribution learning. In *Proceedings of the IEEE/CVF Conference on Computer Vision and Pattern Recognition*, pages 5206–5215, 2022. 2
- [21] Zhihe Lu, Yongxin Yang, Xiatian Zhu, Cong Liu, Yi-Zhe Song, and Tao Xiang. Stochastic classifiers for unsupervised domain adaptation. In *Proceedings of the IEEE/CVF conference on computer vision and pattern recognition*, pages 9111–9120, 2020. 2
- [22] Sharada P Mohanty, David P Hughes, and Marcel Salathé. Using deep learning for image-based plant disease detection. *Frontiers in plant science*, 7:215232, 2016. 6, 11
- [23] Radford M Neal. *Bayesian learning for neural networks*. Springer Science & Business Media, 2012. 2
- [24] Alec Radford, Jong Wook Kim, Chris Hallacy, Aditya Ramesh, Gabriel Goh, Sandhini Agarwal, Girish Sastry, Amanda Askell, Pamela Mishkin, Jack Clark, et al. Learning transferable visual models from natural language supervi-

- sion. In *International conference on machine learning*, pages 8748–8763. PMLR, 2021. [1](#), [2](#), [4](#)
- [25] Julio Silva-Rodriguez, Sina Hajimiri, Ismail Ben Ayed, and Jose Dolz. A closer look at the few-shot adaptation of large vision-language models. In *Proceedings of the IEEE/CVF Conference on Computer Vision and Pattern Recognition*, pages 23681–23690, 2024. [6](#)
 - [26] Jiahe Tian, Cai Yu, Xi Wang, Peng Chen, Zihao Xiao, Jizhong Han, and Yesheng Chai. Dynamic mixed-prototype model for incremental deepfake detection. In *Proceedings of the 32nd ACM International Conference on Multimedia*, pages 8129–8138, 2024. [7](#)
 - [27] Xiaosong Wang, Yifan Peng, Le Lu, Zhiyong Lu, Mohammadhadi Bagheri, and Ronald M Summers. Chestx-ray8: Hospital-scale chest x-ray database and benchmarks on weakly-supervised classification and localization of common thorax diseases. In *Proceedings of the IEEE conference on computer vision and pattern recognition*, pages 2097–2106, 2017. [6](#), [11](#)
 - [28] Kangyu Xiao, Zilei Wang, and Junjie Li. Semantic-guided robustness tuning for few-shot transfer across extreme domain shift. In *European Conference on Computer Vision*, pages 303–320. Springer, 2024. [1](#), [2](#)
 - [29] Hantao Yao, Rui Zhang, and Changsheng Xu. Tcp: Textual-based class-aware prompt tuning for visual-language model. In *Proceedings of the IEEE/CVF Conference on Computer Vision and Pattern Recognition*, pages 23438–23448, 2024. [2](#), [4](#), [6](#), [8](#), [11](#)
 - [30] Tianyuan Yu, Da Li, Yongxin Yang, Timothy M Hospedales, and Tao Xiang. Robust person re-identification by modelling feature uncertainty. In *Proceedings of the IEEE/CVF international conference on computer vision*, pages 552–561, 2019. [2](#)
 - [31] Tao Yu, Zhihe Lu, Xin Jin, Zhibo Chen, and Xinchao Wang. Task residual for tuning vision-language models. In *Proceedings of the IEEE/CVF Conference on Computer Vision and Pattern Recognition*, pages 10899–10909, 2023. [6](#)
 - [32] Kaiyang Zhou, Jingkang Yang, Chen Change Loy, and Ziwei Liu. Learning to prompt for vision-language models. *International Journal of Computer Vision*, 130(9):2337–2348, 2022. [1](#), [2](#), [6](#)
 - [33] Kaiyang Zhou, Chen Change Loy, and Ziwei Liu. Semi-supervised domain generalization with stochastic stylematch. *International Journal of Computer Vision*, 131(9):2377–2387, 2023. [2](#)
 - [34] Yixiong Zou, Yicong Liu, Yiman Hu, Yuhua Li, and Ruixuan Li. Flatten long-range loss landscapes for cross-domain few-shot learning. In *Proceedings of the IEEE/CVF Conference on Computer Vision and Pattern Recognition*, pages 23575–23584, 2024. [1](#), [2](#)
 - [35] Yixiong Zou, Shuai Yi, Yuhua Li, and Ruixuan Li. A closer look at the cls token for cross-domain few-shot learning. *Advances in Neural Information Processing Systems*, 37: 85523–85545, 2025. [2](#)

Supplementary Material

	Aircraft	DTD	Flowers	Caltech101	Food101	Oxford Pets	Average
MaPLe	29.03	54.73	80.80	94.30	86.90	92.05	72.97
PromptSRC	32.80	60.64	91.31	<u>94.77</u>	<u>86.06</u>	93.23	76.47
TCP	<u>36.20</u>	63.97	94.40	95.00	85.30	91.90	77.80
MIST	36.60	<u>61.40</u>	<u>91.73</u>	94.67	82.47	<u>92.80</u>	<u>76.61</u>

Table 6. Performance (%) on the CLIP-based FSL datasets for the 4-shots setting. Highest and second highest values are marked by bold and underline respectively.

A. More Dataset details: We have used the four datasets from the BSCDFSL [10] benchmark to construct our proposed pCDFSL setting. This benchmark consists of images and classnames from various specialized domains like medical, satellite and agricultural fields, displaying extreme domain shifts from natural images. We provide more details on each of these datasets below:

1) **EuroSAT [11]:** This dataset consists of satellite images of various terrains and comprises of 10 classes, namely, Annual Crop, Forest, Herbaceous Vegetation, Permanent Crop, Residential Buildings, Pasture, Industrial buildings, Highway, River, Sea-Lake.

2) **ISIC [5]:** Consists of dermoscopic skin disease images and has 7 classes, namely, Melanoma, Melanocytic Nevi, Basal Cell Carcinoma, Actinic Keratosis, Benign Keratosis, Dermatofibroma, Vascular Lesions.

3) **Plant Disease [22]:** Contains images of leaf diseases across 38 classes, e.g., Apple Scab, Apple Black Rot, Apple Cedar Rust, Apple Healthy, Blueberry healthy, Cherry Powdery Mildew, Cherry Healthy, and so on.

4) **ChestX [27]:** This dataset comprises of greyscale chest X-Ray images across 7 classes, namely, Atelectasis, Cardiomegaly, Effusion, Infiltration, Mass, Nodule, Pneumothorax.

The datasets ranked in decreasing order of similarity with ImageNet [6] are as follows: Plant Disease > EuroSAT > ISIC > ChestX.

B. CLIP-based FSL performance: The detailed results of the few-shot experiments on the CLIP-based FSL datasets are reported in Table 6.

C. Memory consumption: We report the comparative GPU memory consumptions for the 1-shot case in Table 7. Here, we observe that our proposed MIST utilizes slightly more memory than MaPLe [15] during training, due to addition of learnable parameters, but utilizes the same memory during inference. However, PromptSRC [16] takes up much more memory during both training and inference. TCP [29] takes slightly less memory due to

	MaPLe	PromptSRC	TCP	MIST (Ours)
Training	1172	2168	778	1348
Inference	1608	2994	4946	1610

Table 7. Comparison of the GPU memory requirements (in MBs) for training and inference.

fewer learnable parameters during training, but consumes a huge memory during inference, due to loading of the frozen CLIP model. Overall, our proposed MIST framework fairs comparably to MaPLe, and is more suitable for real-world deployment compared to the other methods.